Hardware-Efficient and Fully Autonomous Quantum Error Correction in Superconducting Circuits

Eliot Kapit
Department of Physics and Engineering Physics, Tulane University, New Orleans, Louisiana 70118, USA
and Initiative for Theoretical Science, The Graduate Center, City University of New York, New York, New York 10016, USA
(Received 15 December 2015; published 12 April 2016)

Superconducting qubits are among the most promising platforms for building a quantum computer. However, individual qubit coherence times are not far past the scalability threshold for quantum error correction, meaning that millions of physical devices would be required to construct a useful quantum computer. Consequently, further increases in coherence time are very desirable. In this Letter, we blueprint a simple circuit consisting of two transmon qubits and two additional lossy qubits or resonators, which is passively protected against all single-qubit quantum error channels through a combination of continuous driving and engineered dissipation. Photon losses are rapidly corrected through two-photon drive fields implemented with driven superconducting quantum interference device couplings, and dephasing from random potential fluctuations is heavily suppressed by the drive fields used to implement the multiqubit Hamiltonian. Comparing our theoretical model to published noise estimates from recent experiments on flux and transmon qubits, we find that logical state coherence could be improved by a factor of 40 or more compared to the individual qubit T_1 and T_2 using this technique. We thus demonstrate that there is substantial headroom for improving the coherence of modern superconducting qubits with a fairly modest increase in device complexity.

DOI: 10.1103/PhysRevLett.116.150501

A universal quantum computer could provide enormous computing power [1], but all attempts to construct such a device have been stymied by noise arising from uncontrolled interactions between the physical qubits and their environment. These quantum errors can be mitigated by a quantum error correction [2–6], where a logical bit is encoded in the collective state of a much larger number of physical quantum bits and complex parity-check operations (stabilizers) are repeatedly measured to algorithmically detect or correct errors before they can proliferate. Unfortunately, the overhead requirements for implementing a fault-tolerant quantum code are daunting [4]. To help supplement these complex process, a growing body of work [7–23] has shown that carefully tuned quantum noise, in the form of engineered dissipation, can protect states against the effects of the unwanted noise. However, these approaches introduce their own drawbacks and overhead, and finding the minimal useful implementation—the simplest device which can be built with current technology and passively correct or suppress all single-qubit quantum error channels—has remained an elusive challenge. It is the goal of this Letter to blueprint such a circuit using mature, widely adopted superconducting device technologies.

Loosely inspired by recent proposals for "cat state qubits" in superconducting resonators [18,23,24] and directly adapting the shadow lattice passive error correction architecture previously developed by the author and colleagues [20,21], we propose a logical qubit which could consist of two transmon qubit devices coupled by driven superconducting quantum interference devices (SQUIDs) to each other and to one additional lossy object (either a qubit or resonator) each. By exploiting the particular noise spectra of errors in superconducting qubits, this device demonstrates that passive error correction via resonant energy transfer to a lossy system can dramatically outperform active, measurement-based error correction in small systems, with photon loss error correction rates approaching 10 MHz for realistic device parameters (in contrast to the ∼1 MHz rates from measurement-based methods [25]). Furthermore, it achieves this rapid error correction using a simpler circuit of just two primary qubit devices and two resonators, in contrast to the ten qubits required to correct a single error of any type using the Laflamme code [26], or seventeen qubits for an optimal distance-3 surface code. While dephasing (z noise) is not corrected by this circuit, the continuous drive fields used to implement passive error correction suppress its effects, and we will show that, for decoherence rates observed in modern qubit designs, the effect of z noise here will generally be weaker than that of photon losses. Furthermore, logical gates on or between these qubits are surprisingly simple, and we do not expect them to take significantly longer than gates on or between ordinary transmon qubits.

Basic circuit model.—For clarity and generality, we will consider a simplified theoretical model for our circuit and leave the finer details of an example implementation and the derivation of the various terms to Supplemental Material [27]. We consider a pair of three-level

superconducting qubit devices, labeled by l and r, where the three levels correspond to device occupation by zero, one, or two photons. There is a nonlinearity $-\delta$ for adding a second photon to either device compared to the $0 \to 1$ energy. We couple the two devices via a high-frequency, driven coupling which does not conserve the photon number [28–31] and couple each device via a similar coupling to a second, lossy degree of freedom, such as a rapidly decaying qubit or readout resonator, with a full example circuit shown in Fig. 1. We now make the following operator definitions. We let $P_k^n \equiv |n_k\rangle\langle n_k|$ be the projector onto all states with n photons in object k (and any number of photons in the other parts of the circuit). We further define $\tilde{X}_l \equiv (a_l^\dagger a_l^\dagger + a_l a_l)/2$ and $\tilde{Z}_l \equiv P_l^2 - P_l^0$ (and similarly for r), where a_l annihilates a photon in the left device. We now define our two-device, rotating frame Hamiltonian H_P by

$$H_P = -W\tilde{X}_l\tilde{X}_r + \frac{\delta}{2}(P_l^1 + P_r^1). \tag{1}$$

H_P has two ground states, $\tilde{X}_l = \tilde{X}_r = 1$ or $\tilde{X}_l = \tilde{X}_r = -1$, which we label $|L_0\rangle$ and $|L_1\rangle$ and choose to act as our logical state manifold. This Hamiltonian describes a combination of resonantly driven two-photon exchange and four-photon creation or annihilation for the pair of qubits, with the drives targeting the $|0\rangle \to |2\rangle$ energy (leaving the $|1\rangle$ state detuned). The signal structure which implements this coupling (and the error-correcting two-photon process described below) and the restriction to a three-level basis are described in Supplemental Material [27]. Note that $\tilde{X}_k|1_k\rangle = 0$ due to the three-body constraint.

We now turn to the lossy "shadow" objects, which we will take to be resonators and which we label Sl and Sr (the S label denotes a shadow object, as discussed in [20,21]), with energies ω_{Sl} and ω_{Sr}. The shadow objects are coupled to the primary qubit devices through driven couplings of a different form, yielding the final qubit-resonator Hamiltonian

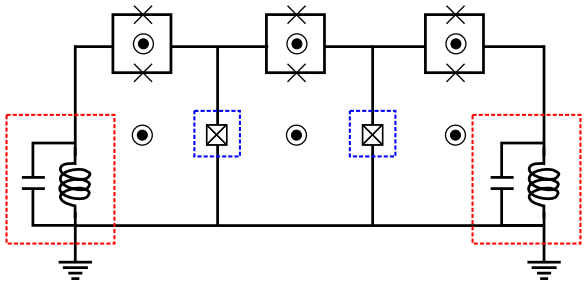

FIG. 1. One possible implementation of our logical qubit. The two transmon qubits (blue boxes) are the good quantum degrees of freedom we wish to protect, and the two readout resonators (red boxes) are lossy objects we will use for error correction. The three driven SQUID couplings have precisely tuned flux biases (black circles) to enable parametric interactions, as discussed in Supplemental Material [27].

$$H_{PS} + H_S = \left(W + \frac{\delta}{2}\right)(a_{Sl}^\dagger a_{Sl} + a_{Sr}^\dagger a_{Sr}) + \Omega(a_l^\dagger a_{Sl}^\dagger + a_r^\dagger a_{Sr}^\dagger + \text{H.c.}). \tag{2}$$

Our final device Hamiltonian is thus $H = H_P + H_{PS} + H_S$. We will now show that, given a resonator decay rate Γ_S which is fast compared to the photon loss rate Γ_P $(= 1/T_1)$ in the two qubits, this circuit is passively protected against all single-qubit errors, leading to exceptionally long coherence for the logical ground states.

Error correction: Photon losses.—We first tackle photon loss errors, a white noise error source which to a good approximation occurs at rates independent of many-body energetics (W terms). Without loss of generality, we consider a single-photon loss in the left qubit, which sends

$$a_l|L_0\rangle \to |1_l\rangle \otimes \frac{|0_r\rangle + |2_r\rangle}{\sqrt{2}} \otimes |0_{Sl}0_{Sr}\rangle,$$
$$a_l|L_1\rangle \to |1_l\rangle \otimes \frac{-|0_r\rangle + |2_r\rangle}{\sqrt{2}} \otimes |0_{Sl}0_{Sr}\rangle. \tag{3}$$

However, these states are not eigenstates of H, due to the qubit-resonator couplings H_{PS}. In the limit $W \gg \Omega$, the full single-photon excited states $|E_{i\pm}\rangle$ are

$$|E_{0\pm}\rangle \equiv \frac{1}{\sqrt{2}}\left[|1_l\rangle \otimes \frac{|0_r\rangle + |2_r\rangle}{\sqrt{2}} \otimes |0_{Sl}0_{Sr}\rangle \pm \frac{|0_l\rangle + |2_l\rangle}{\sqrt{2}} \otimes \frac{|0_r\rangle + |2_r\rangle}{\sqrt{2}} \otimes |1_{Sl}0_{Sr}\rangle\right],$$
$$|E_{1\pm}\rangle \equiv \frac{1}{\sqrt{2}}\left[|1_l\rangle \otimes \frac{-|0_r\rangle + |2_r\rangle}{\sqrt{2}} \otimes |0_{Sl}0_{Sr}\rangle \pm \frac{-|0_l\rangle + |2_l\rangle}{\sqrt{2}} \otimes \frac{-|0_r\rangle + |2_r\rangle}{\sqrt{2}} \otimes |1_{Sl}0_{Sr}\rangle\right]. \tag{4}$$

Consequently, when a photon is lost from $|L_0\rangle$, the quantum system is placed in a superposition of $|E_{0+}\rangle$ and $|E_{0-}\rangle$ and will Rabi flop at rate Ω. However, photons in the shadow resonators rapidly decay, and the resulting a_{SL} operation will return an $|E_0\rangle$ superposition to $|L_0\rangle$ and an $|E_1\rangle$ superposition to $|L_1\rangle$, without any additional phases accumulated in the process. Thus, photon loss errors are rapidly corrected in a manner which preserves superpositions of the two logical states; the energy conservation requirement enforced by $\delta \gg W \gg \Omega$ minimizes any excursions from the logical state manifold due to the error correction and ensures that $|E_0\rangle$ corrects only to $|L_0\rangle$ and $|E_1\rangle$ corrects only to $|L_1\rangle$. However, a second photon loss in either qubit before correction occurs will lead to a logical error. Integrating out the shadow resonators, the "repair" rate $\Gamma_R(\Delta E)$ for a process which changes the two-device system's energy by ΔE is given by

$$\Gamma_R(\Delta E) = \frac{4\Omega^2\Gamma_S}{4\Omega^2 + 4(\Delta E + W + \frac{\delta}{2})^2 + \Gamma_S^2}. \quad (5)$$

Here, Γ_R is maximized when $\Delta E = -W - \delta/2$, which is precisely the energy of correcting a $|E\rangle$ state to its parent $|L\rangle$ state. Noting that there are an average of two photons in the circuit at any time and assuming $\delta \gg W$, we arrive at a net logical error rate from photon losses and off-resonant shadow resonator interactions of

$$\Gamma_E^X \simeq 2\Gamma_R\left(W + \frac{\delta}{2}\right) + \frac{2\Gamma_P(2\Gamma_P + \Gamma_R(+W - \frac{\delta}{2}))}{\Gamma_R(-W - \frac{\delta}{2})},$$
$$\Gamma_E^Y \simeq \frac{2\Gamma_P(2\Gamma_P + \Gamma_R(+W - \frac{\delta}{2}))}{\Gamma_R(-W - \frac{\delta}{2})}. \quad (6)$$

Here, Γ_E^X and Γ_E^Y are the rates of random $\tilde{X}$ or $\tilde{Y}$ operations on a qubit in the circuit. In the limit $W \gg \Omega$, this is $4\Gamma_P^2/\Gamma_R(-W - \frac{\delta}{2})$, which can be dramatically smaller than Γ_P. A random $\tilde{X}$ or $\tilde{Y}$ operation can dephase a logical superposition or flip between logical states. Note that noise in either the W or Ω terms will not significantly degrade the performance of the circuit; fluctuation in the magnitude of W does not dephase logical states and interferes with error correction only if $\delta W \geq \Omega$, which would be a fairly substantial fluctuation. As the Ω term does not distinguish logical states, fluctuation in its amplitude and phase should be similarly harmless.

In Fig. 2, we demonstrate the effectiveness of this protection against photon losses by numerically integrating the Lindblad equations [32] for the system's density matrix ρ. Specifically, given a photon loss rate Γ_P, we have

$$\partial_t\rho = -\frac{i}{\hbar}[H,\rho] + \frac{\Gamma_P}{2}\sum_{j=L,R}(2a_j\rho a_j^\dagger - \{a_j^\dagger a_j, \rho\}) + \frac{\Gamma_S}{2}\sum_{j=L,R}(2a_{Sj}\rho a_{Sj}^\dagger - \{a_{Sj}^\dagger a_{Sj}, \rho\}). \quad (7)$$

As described in the figure caption, we can define two lifetimes for our logical states. The first, T_{1L}, is defined by initializing the system in either logical state and fitting the resulting decay to an incoherent mixture of the two logical states to an exponential decay law. The second, T_{2L}, is a dephasing time defined by initialization to the state $(|L_0\rangle \pm |L_1\rangle)/\sqrt{2}$ and fitting the expectation value of $\tilde{Z}_l\tilde{Z}_r$ to an exponential decay law. We note that T_{2L} will always be less than T_{1L}, as it is sensitive to both Γ_E^X and Γ_E^Y errors (6), where T_{1L} is sensitive only to Γ_E^Y processes. In both cases, we neglect short time transient behavior (time scales less than $1/\Omega$), the effect of which is merged into an overall fidelity multiplier F. This stems from the fact that the system is measured; there is always a small chance of finding it outside of the logical state manifold, as the measurement may occur between a photon loss and its passive correction. This effect leads to a short time dip in the expectation values of the logical operators $\tilde{X}$ and $\tilde{Z}_l\tilde{Z}_r$ after state initialization, where the error rate is $2\Gamma_P$ for an interval of $\Delta t \approx \hbar/\Omega$ and slows down to the predicted rates in (6) after that (we neglect this short time behavior in our numerical fits to estimate lifetimes). However, if the measurement detects a $|1\rangle$ state, a subsequent measurement will capture the original (preloss) state with probability $P \simeq \Gamma_R/(\Gamma_R + 2\Gamma_P)$ due to the continuous passive error correction.

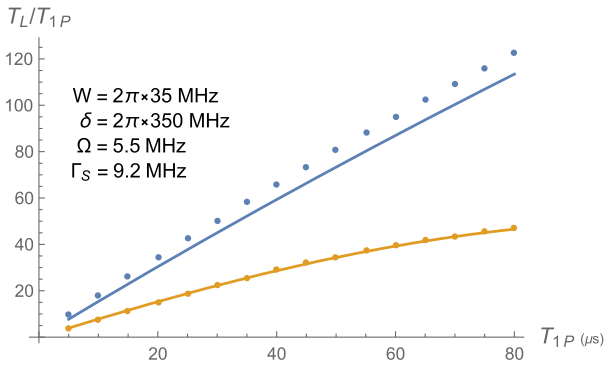

FIG. 2. Strong enhancement of the effective logical state lifetimes T_L against photon losses through engineered dissipation, with all times in microseconds. Each data point is computed by numerically integrating the Lindblad equations for the Hamiltonian $H = H_P + H_S + H_{PS}$ from (1) and (2), with parameters as stated in the plot legend and varying "bare" $T_{1P} \equiv 1/\Gamma_P$ from photon losses in the two primary qubits. The blue points plot the improvement factor T_{1L}/T_{1P}; T_{1L} captures the decay of the system to an incoherent mixture of states after initialization to $|0_L\rangle$, extracted by fitting the measure $\mathrm{Tr}[\rho|0_L\rangle\langle 0_L|]$ to an exponential decay law, with short-term transient behavior dropped. The orange points plot the improvement factor T_{2L}/T_{1P} of the "dephasing" time T_{2L}, extracted by initializing the system to $\tilde{Z}_l\tilde{Z}_r = \pm 1$ and fitting $\mathrm{Tr}[\rho\tilde{Z}_l\tilde{Z}_r]$ (the plotted value is the average of the $\tilde{Z}_l\tilde{Z}_r = +1$ and $\tilde{Z}_l\tilde{Z}_r = -1$ states). The two continuous curves plot the analytically predicted improvement factor from the rates calculated in (6). The lifetime T_{2L} is reduced by the constant error term in Γ_E^X; this term does not limit T_{1L}, as the system is initialized in an $\tilde{X}$ eigenstate. Increasing the nonlinearity δ would raise the limit for T_{2L} improvement by passive error correction. Note that all points on the plot are past the "break-even" point ($T_L = T_{1P}$), which occurs around $T_{1P} \simeq 1$ μs.

Finally, we should consider photon addition. An incoherent photon addition error can immediately lead to a logical error, since it takes $|0\rangle \to |1\rangle$ which is then rapidly converted to $|2\rangle$ by passive error correction, potentially enacting $\tilde{X}$. However, for modern, well-shielded experiments, the available population of thermal photons is vanishingly small, and the random photon addition rate is 2 or more orders of magnitude less than the loss rate [33]. This is thus unlikely to limit our logical state lifetimes.

Error suppression: Dephasing.—Having shown that our circuit is capable of rapidly correcting photon loss errors,

we now demonstrate that the continuously applied many-body Hamiltonian H_P (1) required for error correction has the beneficial side effect of suppressing dephasing noise as well. Unlike the white noise of photon losses, dephasing noise has a power spectrum that is strongly frequency dependent, typically being comprised of $1/f$ and telegraph components [34–41]. The noise power spectra of these two sources are given by

$$S_{1/f} = \frac{2\pi S_0}{\omega}, \qquad S_{\mathrm{tel}} = \frac{(\Delta\omega_{10})^2\Gamma_{sw}}{\pi(\omega^2 + \Gamma_{sw}^2)}. \tag{8}$$

If a system is continuously driven along x, the resulting interference between the effective Hamiltonian term $\eta\sigma^x$ and the fluctuating noise term $\delta z(t)\sigma^z$ can also strongly suppress phase noise [34,35,37,39,41,42]. When considering times $t > \eta^{-1}$, the average phase noise in this Rabi sequence is

$$\langle \phi^2(t)\rangle^{(\mathrm{Rabi})} \simeq \pi S(\eta) t, \tag{9}$$

where η is the Rabi frequency of the drive term ($2\pi \times 35$ MHz in Fig. 2). This leads to exponential rather than Gaussian decay for both types of noise, and the noise suppression from a large η can be dramatic. In our system, the large W term will play exactly the same role, albeit with the noise strength S_0 increased by a factor of 4 relative to the single-qubit noise measure, as we are working with two-photon states and there are two qubits experiencing noise. For a given $T_2^{(\mathrm{echo})}$ from $1/f$ noise, the effective mixing time T_{LZ} in our driven system can be vastly larger; for example, for single-qubit $T_2^{(\mathrm{echo})} = 10\ \mu$s and $W = 2\pi \times 35$ MHz we obtain $T_{LZ} \sim 2$ ms. These results were confirmed to be qualitatively accurate by numerical noise simulations (see Supplemental Material [27]). Since the $1/f\ T_2^{(\mathrm{echo})}$ scales as $1/\sqrt{S_0}$ and our Rabi-driven T_{LZ} scales as $1/S_0$, a linear increase in $T_2^{(\mathrm{echo})}$ from improved shielding or qubit design leads to a quadratic increase in T_{LZ}, just as in the photon loss channel. Similarly, for telegraph noise, $W \gg \Gamma_{sw}$ is readily achievable, and in this limit Rabi driving can outperform spin echo as well. To verify the prediction (9), we simulated dephasing by averaging numerical simulations of randomly telegraph spectra. Within these simulations (included in Supplemental Material [27]), using published data from Ref. [41] we find a range of simulated T_{LZ} values from 0.2 ms for $\{W = 2\pi \times 25, \Gamma_{sw} = 11.9, \Delta\omega_{10} = 2\pi \times 0.48\}$ MHz up to 6 ms for $\{W = 2\pi \times 35, \Gamma_{sw} = 4.96, \Delta\omega_{10} = 2\pi \times 0.2\}$. We thus conclude that logical state lifetimes in the millisecond range are still achievable in the presence of realistic telegraph and $1/f$ noise sources.

We caution that our circuit offers no protection against true white noise dephasing [where $S(\omega)$ is constant at high frequency ranges], and increasing W does not improve T_{LZ} in this case. However, noise of this type is typically extremely weak and sometimes entirely absent in noise spectroscopies of the modern superconducting qubit, with photon losses, flicker, and telegraph noise dominating the error rate. Furthermore, if white noise dephasing becomes a problem, it can be *corrected* by constructing a three-device ring from our circuit and implementing a passive variant of the three-qubit phase flip code [21] alongside the passive photon loss correction.

Finally, we note that single-qubit dephasing is not the only z noise channel in our system, as two-body dephasing is also a concern. Specifically, flux noise through the coupling SQUID loop can lead to a fluctuating $\tilde{Z}_l\tilde{Z}_r$ term [43], though generally with a much smaller coefficient than the accompanying single-qubit $\tilde{Z}$ terms. Because it commutes with $\tilde{X}_l\tilde{X}_r$ and mixes the two logical states, this term is dangerous. Fortunately, however, based on previous experiments with flux qubits (where $1/f$ flux noise through the qubit loop accounts for nearly all of the dephasing [37,39,42]), we expect this noise to be very weak at the symmetry point at which our device is operated, with a typical noise power $A(1\ \mathrm{Hz}) \simeq 1\mu\Phi_0/\sqrt{Hz}$. Assuming $1/f$ noise of this strength and the device parameters in Supplemental Material [27] ($E_J/E_C = 50$, with the two coupling SQUID junctions having energy $E_J = 2\pi \times 15$ GHz), we obtain $T_{ZZ} \simeq 16$ ms as measured by an equivalent protocol to spin echo. More complex constructions can suppress this noise if it ultimately becomes necessary.

Logical gates and conclusion.—A simple universal two-qubit gate set can be implemented by combining single-qubit rotations with the CONTROLLED-Z (CZ) operation. We let either $\tilde{X}$ operator play the role of logical Z (Z_L). To enact single logical qubit rotations, we apply a finite length pulse involving combinations of a temporary phase shift for the signals which generate W drive fields through the central SQUID (enacting $\tilde{Y}_l\tilde{Y}_r$, or X_L) and driving a single device resonantly at the $|0\rangle \leftrightarrow |2\rangle$ transition (enacting $\tilde{X}$, or Z_L). As the g terms do not commute with $\tilde{Y}_l\tilde{Y}_r$, they may have to be briefly adjusted. An appropriately tuned sequence of these terms can rapidly enact arbitrary single-qubit rotations. Since the SQUID coupling can be driven fairly strongly (especially for short, highly tuned pulses), we do not expect these rotations to take significantly longer than in single-qubit devices. To apply the CZ gate, we couple two of these qubit device pairs to each other, again through a driven SQUID coupling. Labeling the two device pairs (logical qubits) by A and B, we simultaneously apply $\tilde{X}_{lA}\tilde{X}_{lB}$ through the coupling SQUID while applying $\tilde{X}_{lB}$ to the left qubit device of the B pair. The sum of the two signals (which must be properly synchronized) run for an appropriate time enacts $I + (1 + Z_{LA})(Z_{LB})/2$, the logical CZ gate. Finally, our logical qubit could be measured along $\tilde{X}$ through a similar driven coupling to a resonator, analogously to the protocol proposed by Didier, Bourassa, and Blais [44].

By considering a simple two-qubit circuit with driven couplings and two auxiliary lossy objects, we have demonstrated that passive error correction can lead to large improvements in qubit coherence against all common error channels with current technology. While our device is capable of only correcting or suppressing a single error at a time, it does so very rapidly and permits simple and rapid logical gates between devices. We would like to develop a way to systematically integrate this logical bit into larger measurement-based codes, and future study of hybrid quantum error correction (QEC) codes, where active and passive QEC methods work in concert, could be an extremely fruitful line of research.

We thank Michel Devoret, Eric Holland, Jens Koch, Vadim Oganesyan, David Pappas, and David Schuster for useful discussions. This work was supported by Tulane University and by the Initiative for Theoretical Science at the Graduate Center of the City University of New York.

[1] M. A. Nielsen and I. L. Chuang, *Quantum Computation and Quantum Information: 10th Anniversary Edition* (Cambridge University Press, Cambridge, England, 2011).
[2] A. Kitaev, Ann. Phys. (Amsterdam) **303**, 2 (2003).
[3] H. Bombin, Phys. Rev. A **81**, 032301 (2010).
[4] A. G. Fowler, M. Mariantoni, J. M. Martinis, and A. N. Cleland, Phys. Rev. A **86**, 032324 (2012).
[5] X.-C. Yao *et al.*, Nature (London) **482**, 489 (2012).
[6] B. Terhal, Rev. Mod. Phys. **87**, 307 (2015).
[7] J. F. Poyatos, J. I. Cirac, and P. Zoller, Phys. Rev. Lett. **77**, 4728 (1996).
[8] S. Diehl, A. Micheli, A. Kantian, B. Kraus, H. P. Büchler, and P. Zoller, Nat. Phys. **4**, 878 (2008).
[9] B. Kraus, H. P. Büchler, S. Diehl, A. Kantian, A. Micheli, and P. Zoller, Phys. Rev. A **78**, 042307 (2008).
[10] F. Verstraete, M. M. Wolf, and J. I. Cirac, Nat. Phys. **5**, 633 (2009).
[11] F. Pastawski, A. Kay, N. Schuch, and I. Cirac, Quantum Inf. Comput. **10**, 580 (2010).
[12] F. Pastawski, L. Clemente, and J. I. Cirac, Phys. Rev. A **83**, 012304 (2011).
[13] Karl Gerd H. Vollbreht, C. A. Muschik, and J. I. Cirac, Phys. Rev. Lett. **107**, 120502 (2011).
[14] K. W. Murch, U. Vool, D. Zhou, S. J. Weber, S. M. Girvin, and I. Siddiqi, Phys. Rev. Lett. **109**, 183602 (2012).
[15] M. J. Kastoryano, M. M. Wolf, and J. Eisert, Phys. Rev. Lett. **110**, 110501 (2013).
[16] S. Shankar, M. Hatridge, Z. Leghtas, K. M. Sliwa, A. Narla, U. Vool, S. M. Girvin, L. Frunzio, M. Mirrahimi, and M. H. Devoret, Nature (London) **504**, 419 (2013).
[17] C. Aron, M. Kulkarni, and H. E. Türeci, Phys. Rev. A **90**, 062305 (2014).
[18] M. Mirrahimi, Z. Leghtas, V. V. Albert, S. Touzard, R. J. Schoelkopf, L. Jiang, and M. H. Devoret, New J. Phys. **16**, 045014 (2014).
[19] J. Cohen and M. Mirrahimi, Phys. Rev. A **90**, 062344 (2014).
[20] E. Kapit, M. Hafezi, and S. H. Simon, Phys. Rev. X **4**, 031039 (2014).
[21] E. Kapit, J. T. Chalker, and S. H. Simon, Phys. Rev. A **91**, 062324 (2015).
[22] S. Hacohen-Gourgy, V. Ramasesh, C. D. Grandi, I. Siddiqi, and S. M. Girvin, Phys. Rev. Lett. **115**, 240501 (2015).
[23] Z. Leghtas *et al.*, Science **347**, 853 (2015).
[24] L. Sun *et al.*, Nature (London) **511**, 444 (2014).
[25] J. Kelly *et al.*, Nature (London) **519**, 66 (2015).
[26] R. Laflamme, C. Miquel, J. P. Paz, and W. H. Zurek, Phys. Rev. Lett. **77**, 198 (1996).
[27] See Supplemental Material at http://link.aps.org/supplemental/10.1103/PhysRevLett.116.150501 for a detailed consideration of the signal structure, physical Hilbert space, and noise processes of a realistic implementation of this circuit in transmon qubits.
[28] E. Zakka-Bajjani, F. Nguyen, M. Lee, L. R. Vale, R. W. Simmonds, and J. Aumentado, Nat. Phys. **7**, 599 (2011).
[29] E. Kapit, Phys. Rev. A **92**, 012302 (2015).
[30] A. J. Sirois, M. A. Castellanos-Beltran, M. P. DeFeo, L. Ranzani, F. Q. Lecocq, R. W. Simmonds, J. D. Teufel, and J. Aumentado, Appl. Phys. Lett. **106**, 172603 (2015).
[31] K. M. Sliwa, M. Hatridge, A. Narla, S. Shankar, L. Frunzio, R. J. Schoelkopf, and M. H. Devoret, Phys. Rev. X **5**, 041020 (2015).
[32] C. Gardiner and P. Zoller, *Quantum Noise: A Handbook of Markovian and Non-Markovian Quantum Stochastic Methods with Applications to Quantum Optics* (Springer, New York, 2004).
[33] X. Y. Jin *et al.*, Phys. Rev. Lett. **114**, 240501 (2015).
[34] J. M. Martinis, S. Nam, J. Aumentado, K. M. Lang, and C. Urbina, Phys. Rev. B **67**, 094510 (2003).
[35] G. Ithier *et al.*, Phys. Rev. B **72**, 134519 (2005).
[36] F. Yoshihara, K. Harrabi, A. O. Niskanen, Y. Nakamura, and J. S. Tsai, Phys. Rev. Lett. **97**, 167001 (2006).
[37] J. Bylander, S. Gustavsson, F. Yan, F. Yoshihara, K. Harrabi, G. Fitch, D. G. Cory, Y. Nakamura, J.-S. Tsai, and W. D. Oliver, Nat. Phys. **7**, 565 (2011).
[38] S. M. Anton *et al.*, Phys. Rev. B **85**, 224505 (2012).
[39] F. Yan, S. Gustavsson, J. Bylander, X. Jin, F. Yoshihara, D. G. Cory, Y. Nakamura, T. P. Orlando, and W. D. Oliver, Nat. Commun. **4**, 2337 (2013).
[40] E. Paladino, Y. M. Galperin, G. Falci, and B. L. Altshuler, Rev. Mod. Phys. **86**, 361 (2014).
[41] P. J. J. O'Malley *et al.*, Phys. Rev. Applied **3**, 044009 (2015).
[42] F. Yan *et al.*, arXiv:1508.06299.
[43] Static $\tilde{Z}_l\tilde{Z}_r$ terms are not a serious concern, so long as they are known to the experimenter and small compared to W and Ω.
[44] N. Didier, J. Bourassa, and A. Blais, Phys. Rev. Lett. **115**, 203601 (2015).